

Drosophila Brainbow: a recombinase-based fluorescence labeling technique to subdivide neural expression patterns

Stefanie Hampel^{1,2}, Phuong Chung^{1,2}, Claire E McKellar¹, Donald Hall¹, Loren L Looger¹ & Julie H Simpson¹

We developed a multicolor neuron labeling technique in *Drosophila melanogaster* that combines the power to specifically target different neural populations with the label diversity provided by stochastic color choice. This adaptation of vertebrate Brainbow uses recombination to select one of three epitope-tagged proteins detectable by immunofluorescence. Two copies of this construct yield six bright, separable colors. We used *Drosophila* Brainbow to study the innervation patterns of multiple antennal lobe projection neuron lineages in the same preparation and to observe the relative trajectories of individual aminergic neurons. Nerve bundles, and even individual neurites hundreds of micrometers long, can be followed with definitive color labeling. We traced motor neurons in the subesophageal ganglion and correlated them to neuromuscular junctions to identify their specific proboscis muscle targets. The ability to independently visualize multiple lineage or neuron projections in the same preparation greatly advances the goal of mapping how neurons connect into circuits.

The ability to label individual neurons in their entirety and to trace their dendritic and axonal processes in the brain has been a critical neuroanatomical underpinning for studies of how neural circuits drive behavior. Original techniques for neuron labeling included Golgi staining and dye injection¹. Modern methods in *D. melanogaster* have made use of genetic tools, from *lacZ* enhancer trapping to binary expression systems such as upstream activating sequence (*UAS*)-*GAL4* that allow precise targeting of exogenous reporters to defined groups of neurons^{2,3}. It is possible to target individual neurons or groups related by common origin (neuronal lineages made up of the progeny of a given neuroblast stem cell) using stochastic recombination events with mosaic analysis with repressible cell markers (MARCM) or 'Flp-out' techniques. The ability to dissect complex expression patterns by labeling multiple individual neurons or lineages with different colors facilitates the study of how neurons interact with each other. Combinations of fluorescent reporters controlled by different binary expression systems⁴ and twin-spot MARCM⁵

have made it possible to visualize two populations of neurons in different colors. The Brainbow technique^{1,6}, a strategy for labeling many neurons in a mouse brain with distinct fluorescent colors, had enabled analysis of how different neurons interact and visualization of individual neurons in relation to each other in the same preparation.

We combined one of the multicolor labeling techniques of Brainbow (Brainbow-1) with the genetic targeting tools from *Drosophila melanogaster* to differentiate lineages and individual neurons in the same brain. We systematically tested fluorescent proteins in the adult fly brain to choose optimal color combinations. We also developed a variation of the Brainbow technique that relies on antibody labeling of epitopes rather than endogenous fluorescence; this amplifies weak signal to trace fine processes over long distances. The use of spectrally discrete, photostable, narrow-bandwidth small-molecule dyes also makes color assignment much simpler than with the broad excitation and emission spectra of fluorescent proteins. This approach (dBrainbow) speeds up characterization of individual neurons and allows examination of individual cells in relation to each other. These features make it possible to address outstanding questions about how lineages contribute to neural circuits and about how the neurites of adjacent cells partition the areas they innervate in a stereotyped manner. We validated dBrainbow by comparing our results to published findings about antennal lobe projection neuron lineages and single octopaminergic neurons. Then we used dBrainbow to map individual motor neuron cell bodies in the subesophageal ganglion to their proboscis muscle targets.

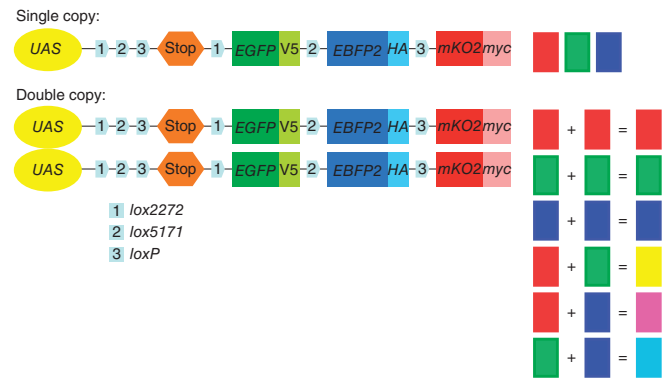
RESULTS

Construct design and optimization of fluorescence

dBrainbow consists of a reporter construct that can be targeted to particular groups of neurons and can then randomly generate one of four outcomes: no color, green fluorescence, red fluorescence or blue fluorescence. The construct (Fig. 1) contains a transcriptional stop sequence followed by genes encoding three cytoplasmic fluorescent proteins. These four cassettes are flanked by pairs

¹Janelia Farm Research Campus, Howard Hughes Medical Institute, Ashburn, Virginia, USA. ²These authors contributed equally to this work. Correspondence should be addressed to J.H.S. (simpsonj@janelia.hhmi.org).

Figure 1 | Schematic of the *dBrainbow* construct. *UAS-dBrainbow* contains a *UAS* that allows its expression to be cell-specifically controlled by the presence of GAL4. Cre recombination occurs only between matched *lox* sites. The selection of *lox* site recombination in a given cell is stochastic. In the absence of recombinase, no fluorescent proteins are made because of a stop cassette with three-frame translation terminators and an SV40 polyadenylation signal. Recombination between *lox2272* sites removes this stop cassette and permits expression of EGFP-V5; recombination between the *lox5171* sites results in expression of EBFP2-HA; and recombination between *loxP* sites produces mKO2-Myc. Cre-mediated recombination is irreversible. Colors from one or two copies of *UAS-dBrainbow* are shown on the right. All fluorescent proteins are cytoplasmic and epitope-tagged as indicated.



of mutually exclusive *lox* sites that function in *D. melanogaster*. In the presence of Cre recombinase, recombination occurs between one of the matched pairs of *lox* sites and results in the irreversible selection of one of the fluorescent proteins. The *UAS-dBrainbow* construct is inserted into defined loci on the second and third chromosomes (*attP2* and *attP40*); fly stocks carrying both chromosomes allow the production of six color combinations (Fig. 1).

We used the same construct for imaging live samples with endogenous fluorescence and fixed samples using fluorescently labeled antibodies to the epitopes attached to each fluorescent protein (Fig. 2). Live imaging requires bright, photostable, spectrally separable fluorescent proteins. Derivatives of green and red fluorescent proteins (GFP and dsRed or mRFP) are commonly used in flies. In an extensive search for additional spectrally separable fluorescent proteins (Supplementary Table 1 and Supplementary Fig. 1) we identified a superior orange-red fluorescent protein, mKO2 (ref. 7) but could not find proteins with good endogenous fluorescence emission in either blue or far-red wavelength range. We nonetheless tried EBFP2 (ref. 8) with EGFP and mKO2 and constructed *UAS-dBrainbow* (Fig. 1). An unfixed brain with a single copy of *UAS-dBrainbow* expressed in three projection neuron lineages of the adult antennal lobe showed separable red and green fluorescence even in small neurites, but blue was only weakly detectable (Fig. 2a–d). This led us to focus our optimization efforts on the use of epitope tags and antibodies. In the future, improvements in fluorescent proteins may provide better options for imaging endogenous fluorescence.

Epitope tags and antibodies allow spectral separation

We needed (i) small epitopes expressible as fusions to soluble proteins, (ii) primary antibodies that recognize these epitopes with high affinity and specificity and can penetrate fixed tissue well, and (iii) secondary antibodies labeled with bright, spectrally discrete dyes (for example, Alexa Fluors). Although there are many antibody-epitope combinations available for biochemical applications, only a few are routinely used for *D. melanogaster* immunohistochemistry. A major limitation for simultaneous color visualization is the number of distinct species in which primary antibodies are available. We explored primary antibodies generated in mouse, rabbit, rat, goat and chicken (Supplementary Table 2 and Supplementary Fig. 2). We used antibodies that performed well in a *GAL4* line with strong expression (*GH146-GAL4* line) and on a sparser line (*a81-GAL4* line; enhancer trap in *CG13432*; J.H.S., unpublished data) to provide a more stringent test; some of the antibodies (antibodies to V5 and hemagglutinin (HA)

epitopes) performed as well as the widely used antibodies to GFP and to CD8 (Supplementary Fig. 3). In addition to allowing the best options to be selected for the *dBrainbow* construct, this effort expands the options for other experiments that require multiple distinctly labeled transgenes to be imaged in the same fly.

We selected the V5, HA and Myc epitopes for the *UAS-dBrainbow* construct (Fig. 1). Because we observed endogenous fluorescence, especially from mKO2, that survived the longer fixation for the epitope staining procedure, we chose secondary antibodies in the same spectral domain as the endogenous fluorescent proteins. Antibody staining of flies expressing *UAS-dBrainbow* in olfactory projection neurons revealed three distinct colors (Fig. 2e–h). For applications involving fixed tissue, the antibody-based method had superior performance to detection of endogenous fluorescence.

It is possible to combine endogenous fluorescence and antibody-based staining in the same preparation. Endogenous orange-red fluorescence from mKO2 can be combined with antibody staining for EGFP, EBFP2-HA and the neuropil marker nc82 (Fig. 2i–k). This results in four distinct imaging channels and allows the inclusion of a neuropil reference marker to assist in identifying unlabeled glomeruli or for registering different preparations onto a common coordinate system.

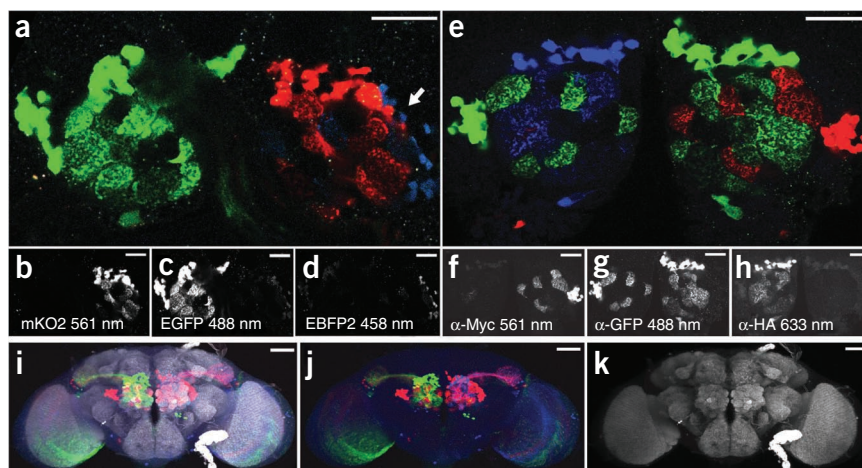
Subdividing complex *GAL4* expression patterns

GAL4 lines that target expression of reporters to specific groups of neurons have been instrumental for dissecting neuroanatomy and connectivity within the fly brain but often produce complex expression patterns. As it is unlikely that individual neurons are uniquely specified by their gene expression profiles alone, there is a limit to the cellular resolution the *GAL4* lines can provide. Random FLP-out methods can be used to subdivide these patterns⁹ but results from different flies must then be compared to reconstruct the entire pattern. Combining *GAL4* lines with the stochastic color choice of *UAS-dBrainbow* enables neuron-by-neuron subdivision in the same preparation.

To validate *dBrainbow*, we used the well-studied projection neurons of the olfactory system. The antennal lobe is the first processing region of the adult olfactory system and comprises distinct glomerular structures, each of which receive inputs from neurons carrying a specific olfactory receptor type; projection neurons innervate individual or combinations of glomeruli and send neurites to the mushroom body calyx and lateral horn¹⁰. MARCM and FLP-out experiments have shown that these projection neurons belong to distinct developmental lineages that partition the antennal lobe in a stereotyped and non-overlapping fashion^{11–14}. The *dBrainbow* technique allowed us to visualize

Figure 2 | Comparison of endogenous and antibody-based fluorescence of *UAS-dBrainbow* flies.

(a–d) Projections of two 1- μ m slices through the antennal lobes from adult brains of *hs-Cre; GH146-GAL4; UAS-dBrainbow* flies, imaged without fixation. Merged image (a) reveals endogenous fluorescence of EGFP (green), mK02 (red) and EBFP2 (blue; arrow); there is some bleed-through into the GFP channel. Raw grayscale images show mK02 (b), EGFP (c) and EBFP2 (d) fluorescence; laser wavelengths are indicated in the images. (e–h) Flies of the same genotype were fixed and stained with primary antibodies to GFP (α -GFP), Myc (α -Myc) and HA (α -HA), and secondary antibodies coupled to Alexa Fluors 488, 568 and 633, respectively. Merged image (e) shows all three colors and individual images (f–h) show spectral separation of Alexa Fluor dyes and lack of antibody cross-reactivity. (i–k) Maximum intensity projections of 20 \times confocal stacks for whole brains labeled with the nc82 antibody as a neuropil marker (gray), with antibodies to GFP (green) and HA (blue), and showing mK02 endogenous fluorescence (red). Merged image (i), EGFP, mK02 and EBFP signals alone (j), and nc82 signal alone (k) are shown. Scale bars, 50 μ m.



the tiled projection neuron patterns in single flies and made this conclusion intuitive (Fig. 3a–f).

GAL4 lines that target each lineage exclusively are not yet available for these projection neurons. *GH146-GAL4*, an enhancer trap inserted near *Oaz*, drives expression in a subset of projection neurons from three different lineages: anterior-dorsal projection neuron (adPN), lateral projection neuron (IPN) and ventral projection neuron (vPN)¹⁴. We crossed *hs-Cre; GH146-GAL4* flies to *UAS-dBrainbow* flies. The *hs-Cre* transgene is thought to be constitutively and ubiquitously expressed even in the absence of heat shock^{15,16}, *dBrainbow* recombination likely occurs in neuroblasts that give rise to daughter cells expressing the same fluorescent protein. With our procedure neurons in each lineage are labeled in the same color, which is ideal for studying the relationships between lineages. In approximately one-third of our preparations, each lineage was labeled in a different color: the choice of color was random, independent and approximately equally distributed (Supplementary Table 3). The adPN and IPN lineages (Fig. 3b) projected to distinct sets of glomeruli: there was no overlap between their neurites. The vPN lineage (Fig. 3a), which had only six cells that express *GH146-GAL4*, also had a distinct projection

pattern. With *dBrainbow* color labeling, we could visualize how the different projection neuron lineages tile the antennal lobe and also how their neurites subdivide the lateral horn. The neurites from the adPN lineage remained segregated from those of the IPN lineage as they traveled to the calyx and lateral horn (Fig. 3g–k), in agreement with published results^{11,14,17}. Because of the bright labeling and unambiguous color assignment, we also could trace neural processes over long distances: single axons from vPN took an alternative route from the antennal lobe to the lateral horn¹⁸ (Fig. 3h).

Two copies of *dBrainbow* increase the color palette

The projection neuron lineages can be subdivided by including a second copy of the *UAS-dBrainbow* transgene: this results in six colors (Fig. 1). The amplification of weak signal by antibody staining makes the presence of a given cassette unambiguous. For our data, we pseudocolored the grayscale photomultiplier signals from the individual red, green and blue color channels established by different excitation laser/emission filter combinations in red, green and blue, respectively, for single copy of the transgene. With two copies, cyan (blue and green), magenta (red and

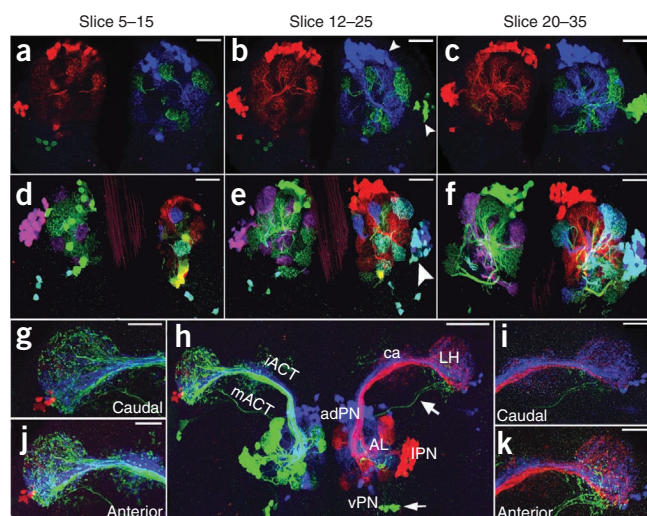


Figure 3 | Expression of *UAS-dBrainbow* in three projection neuron lineages. (a–k) Single (a–c) and double (d–f) copies of *UAS-dBrainbow* were used along with *hs-Cre; GH146-GAL4* to label the three projection neuron lineages that express *GH146-GAL4* (adPN, IPN and vPN) as well as the axon tracts (iACT and mACT) that connect the projection neuron cell bodies to the lateral horn (LH) (h) and calyx (ca) (g,i–k). Shown are maximum intensity projections of several 1- μ m confocal sections (a–f) with each projection neuron lineage expressing a different fluorescent protein–epitope cassette and thus pseudocolored differently (arrowheads; b). The number and depth of confocal slices used to produce the merged images are indicated. In the right IPN lineage (arrowhead; e), recombination in the neuroblast occurred to select blue in one copy of *UAS-dBrainbow* but the recombinase did not act on the second copy until later to select green, so a subset of later-born neurons is labeled in cyan. In h, the antennal lobe (AL) and efferent neurons projecting to the lateral horn via the mACT and iACT; individual neurites can also be traced from the antennal lobe to the lateral horn via an alternative pathway (arrows). Higher-magnification views of the lateral horn from different orientations (g,i–k). Scale bars, 50 μ m (a–f, h) and 20 μ m (g,i–k).

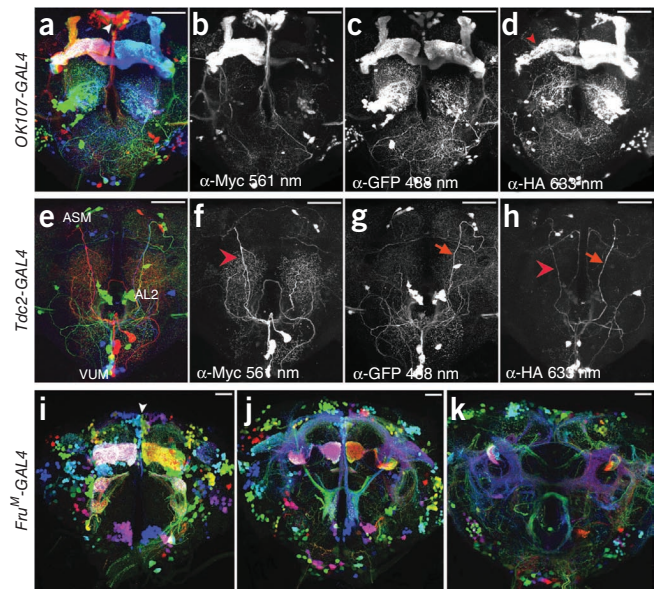
Figure 4 | dBrainbow labeling of lineages or individual neurons in different colors. (a–h) Maximum intensity projections of confocal stacks of *OK107-GAL4* (a–d) and *Tdc2-GAL4* (e–h) with *UAS-dBrainbow* and *hs-Cre* shown as merged images (a,e) and grayscale red (b,f), green (c,g) and blue (d,h) channels, with the imaged wavelengths indicated (blue was used to represent the Alexa Fluor 633). Arrows and arrowheads trace individual ventral unpaired medial (VUM) neurons (f–h). ASM, anterior superior medial protocerebrum and AL2, anterior lateral cluster 2. Arrowhead in d indicates gamma lobe of the mushroom body. (i–k) Three 35- μ m substacks of *hs-Cre; UAS-dBrainbow; UAS-dBrainbow, Fru^M-GAL4* divide the ~2,000 neurons labeled by *Fru^M-GAL4* into many subpopulations, demarcated by different colors. Arrowhead in i indicates the pars intercerebralis. Scale bars, 50 μ m.

blue) and yellow (green and red) were also possible (Fig. 3d–f). Usually a projection neuron lineage was labeled with a single color, but sometimes the recombinase acted on one of the *dBrainbow* constructs partway through neuroblast divisions and a subset of the lineage is labeled in a different color (Fig. 3e): a subset of cyan (blue and green) IPN neurons were nested in a blue IPN lineage clone. This fortuitous temporal delay conferred the ability to subdivide individual lineages and follow their processes in the context of their neighbors.

We used *UAS-dBrainbow* to subdivide the *OK107-GAL4*, *Tdc2-GAL4* and *Fru^M-GAL4* expression patterns, with *Fru^M* encoding the male-specific isoform of the Fruitless transcription factor (Fig. 4). *OK107-GAL4* is expressed in the mushroom bodies¹⁹, intrinsic interneurons of the antennal lobe and many other neurons. Using dBrainbow we labeled the four neuroblasts that compose the mushroom bodies in different colors (Fig. 4a–d). Each neuroblast can produce the three types of mushroom body neurons¹⁹; the time at which the recombination event occurred dictates what mixture of γ , α' β' or α β neurons are labeled in a given color. In some cases (5 of 40 examples) we saw clones that labeled the γ lobes only (Fig. 4d). As these were the first-born neurons, we suspect that the Cre recombinase may prevent neural proliferation or cause toxicity in later-born mushroom body neurons, as has been reported previously¹⁶. When we heat-shocked *hs-Cre; OK107-GAL4; UAS-dBrainbow* flies during development, mushroom body labeling was reduced (data not shown), presumably because more neurons are died or did not develop. To try to obtain a better mixture of colors in each lineage and reduce Cre recombinase toxicity, we identified additional sources of Cre recombinase: *hs-Cre** (ref. 20), *hsp70-Cre*²¹ and *UAS-EBD-Cre*¹⁶. Our results (Supplementary Fig. 4 and data not shown) agreed with the published assessment: all the Cre lines tested were both leaky and incompletely inducible. In *OK107-GAL4* lines, two lineages of antennal lobe intrinsic neurons were also labeled and appeared to project to an overlapping set of glomeruli (Fig. 4a). Both *OK107-GAL4* and *Fru^M-GAL4* express in neurons of the pars intercerebralis. This structure includes neurons that release neuropeptides such as *Drosophila* insulin-like peptides (Dilp) and Phe-Met-Arg-Phe (FMRP)²². Because of the extensive color diversity, our images demonstrated that the pars intercerebralis may include neurons from several different lineages (Fig. 4a,i).

Tracing individual neurons

Octopamine is a biogenic amine that modulates fly aggression, ovulation and appetitive learning²³. There are ~100 broadly projecting octopaminergic neurons marked by *Tdc2-GAL4* expression



in the adult brain, which have been divided into 27 neural cell types based on FLP-out analysis⁹. One of the challenges of prior work was assigning individual cell clones from different specimens to a particular class. Neurons in the same class show variability in different flies²⁴ and some classes have similar projection patterns. *UAS-dBrainbow* allowed us to visualize several individual neurons simultaneously in the same preparation (Fig. 4e–h). With color labeling it is easier to distinguish the ipsilateral projections of the ventral paired median (VPM) neurons from bilateral projections of the ventral unpaired median (VUM) neurons, for example. Based on the FLP-out analysis researchers proposed that there is a single VUM-3a neuron in each of the mandibular and maxillary clusters that has a very similar trajectory²⁴; our results confirmed this because we saw the two neurons in different colors in the same sample. Our images consistently labeled all cells in the anteriolateral cluster (AL2) in a given hemisphere in the same color, suggesting that these neurons derive from the same lineage. Previous work showed that the VPM and VUM neurons derive from distinct lineages²⁴, but in our images the VUM neurons were always labeled in a mixture of colors, indicating that they may derive from several different lineages. It is possible to trace individual axons over long distances, but comparison between the FLP-out clones (with membrane-targeted reporters) and our images suggests that small neurites were not filled as well by the cytoplasmic fluorescent proteins of dBrainbow.

Fru^M is critical in establishing proper male courtship behavior. *Fru^M* expression is complex, including many cell types and more than 2,000 cells^{25,26}. The pattern has been previously subdivided into clusters based on proximity of cell bodies²⁷, but our images (Fig. 4i,k) showed that these clusters are often subdivided by color and thus may include neurons from several different lineages and functional neural classes. Our lineage dissection of the *Fru^M* expression pattern with dBrainbow can now be compared to recent MARCM analysis^{28,29}.

Color labeling aids mapping from brain to periphery

To test dBrainbow for following individual neurons, we applied the technique to motor neurons controlling feeding behavior.

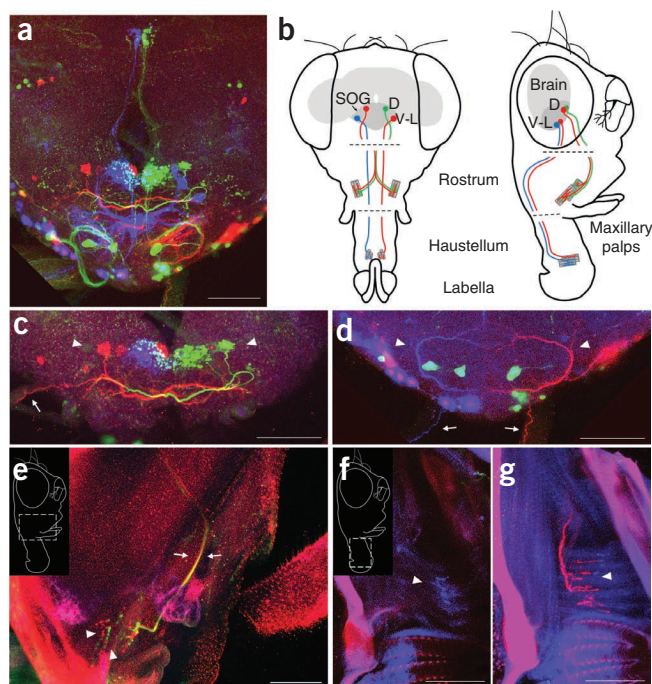


Figure 5 | Expression of *UAS-dBrainbow* in motor neurons that connect the subesophageal ganglion to the proboscis muscles in sections of a single example of an *hs-cre; UAS-dBrainbow; R12D05-GAL4* fly. **(a)** Maximum projection confocal stack showing a cluster of several cell types in the subesophageal ganglion. **(b)** Frontal and lateral schematics of a fly head with proboscis extended, showing brain in gray and subesophageal ganglion (SOG) in darker gray. Two motor neuron types (D and V-L pairs) project to neuromuscular junctions on proboscis muscles. Proboscis was dissected separately (dashed lines) to allow antibody penetration. **(c)** Confocal substack showing dorsal motor neurons in red and green (arrowheads) that send axons out the pharyngeal nerve (arrow). Neurites in the middle do not belong to these neurons as they are labeled in blue and green. **(d)** Confocal substack showing a pair of ventrolateral neurons with C-shaped arbors in the SOG in blue and red (arrowheads). Axons exit via labial nerves (arrows). **(e)** Confocal substack of the rostrum, lateral view, as shown in the inset. The red and green axons travel through the proboscis together (arrows), to terminate at neuromuscular junctions near the distal end of the rostrum (arrowheads). Background was caused by autofluorescence of intact cuticle. **(f,g)** Blue and red axons terminate in neuromuscular junctions on the transverse muscles in the distal end of the haustellum. Substacks at different levels show faint blue **(f)** and bright red **(g)** terminals (arrowheads). At higher gain **(g)**, autofluorescence in the blue channel also shows the muscle fibers of the haustellum: longitudinal muscles (vertical fibers in the image) and transverse muscles (horizontal). Scale bars, 50 μ m.

The subesophageal ganglion at the base of the brain receives gustatory inputs and sends motor outputs to mouthpart muscles. Whereas taste inputs are relatively well studied^{30,31}, questions remain about the function of subesophageal ganglion motor neurons. Retrograde labeling experiments identified several subesophageal ganglion motor neurons innervating proboscis muscles³², but only two types of subesophageal ganglion motor neurons have been thoroughly described with *GAL4* lines and confocal imaging^{33,34}. We analyzed *R12D05-GAL4* transgenic fly line (gift of G. Rubin, Janelia Farm Research Campus) with *dBrainbow* to discover additional motor neurons within a pattern of other cells in the subesophageal ganglion and their muscle targets in the proboscis (**Fig. 5a**).

Because *R12D05-GAL4* expression is relatively sparse and does not contain large lineages, one copy of *dBrainbow* was sufficient for us to identify samples in which the color combinations revealed specific cell types, such as the red-green pair of motor neurons in the dorsal subesophageal ganglion that extend axons ipsilaterally through the pharyngeal nerve and terminate in neuromuscular junctions at the distal end of the rostrum, possibly on muscle 3 (ref. 35). (**Fig. 5**). In nine samples examined, the colors of these two dorsal subesophageal ganglion motor neurons always matched the colors at these neuromuscular junctions (**Supplementary Table 4**). When we crossed the *R12D05-GAL4* line to the *UAS-dBrainbow* line, we observed labeling of a ventrolateral motor neuron pair (**Fig. 5b,d,f,g**) that exits the subesophageal ganglion via the labial nerve. The C-shaped arbors resembled a motor neuron previously characterized by backfilling and attributed to a longitudinal muscle in the haustellum (muscle 6)³². Our color-matching neuromuscular junctions were reproducibly located on the nearby transverse muscle 8, which is suspected to be involved in opening the labella for feeding³⁵. It is possible that *dBrainbow* and three-dimensional confocal imaging will allow more definitive mapping of motor targets than the backfill technique. The two neuron pairs discussed above are the only motor neurons that reproducibly showed neuromuscular junctions in the proboscis in *R12D05-GAL4*. The distinctive arbors of the dorsal and ventrolateral motor

neurons (**Fig. 5b**) were present in most brains examined; counts of these and other subesophageal ganglion cells labeled with *UAS-dBrainbow* in this *GAL4* line are shown in **Supplementary Table 4**. The function of these motor neurons can now be addressed with the genetic access that this *GAL4* line provides.

We thus found that *dBrainbow* can be used to follow arbors of individual neurons in a pattern that would be irresolvable if labeled with a single fluorescent protein. Using *dBrainbow* we labeled neurons from soma and dendrites all the way out through the periphery to neuromuscular junctions. To our knowledge, this is the first account of a *GAL4* line targeting the proboscis motor neurons described here. Having a three-dimensional image of a motor neuron controlling a particular muscle is an important step in understanding the anatomy of circuits underlying motor behaviors.

DISCUSSION

The *Drosophila* Brainbow technique enabled observation of the projections of many different neurons individually in their native context and allowed interactions between lineages to be visualized in the same brain rather than relying on computational alignments of neurons or lineages from different preparations. The combination of neuronal targeting with sparse *GAL4* lines and faithful color expression throughout neurites allowed us to follow processes over long distances and even through discontinuous samples such as the brain and peripheral neuromuscular junction in the proboscis.

The *dBrainbow* construct can be used in two modes: for live imaging with two useable colors from endogenous fluorescence and for imaging fixed tissue with six colors derived from antibody-epitope combinations. To accomplish this, we expanded the repertoire of fluorescent proteins and epitope-antibody options usable in flies. Live imaging using endogenous fluorescence may be best suited to the more transparent embryonic or larval stages. Developments in bright, photostable blue and far-red fluorescent proteins should be incorporated.

The vertebrate Brainbow system was a leap forward in visualizing many individual neurons simultaneously; it allowed direct comparisons between similar neurons in their native context. dBrainbow adds two innovations. First, because the *dBrainbow* construct is under the control of a binary expression system, it can be targeted to neurons of interest using the extensive collections of available *GAL4* lines. (The vertebrate Brainbow is currently fused to a single *Thy1* promoter and so can only be used to visualize neurons in the *Thy1* expression pattern⁶.) Second, the use of epitopes and antibodies permits signal amplification and spectrally discrete, photostable fluorescent dyes. This makes color assignment and fine process tracing easier. Future versions may use membrane-targeted proteins to improve neurite tracing. A synaptically localized version of *dBrainbow* would also have applications for circuit mapping. The *UAS-dBrainbow* construct can be used to anatomically subdivide complex *GAL4* patterns and study individual neurons and lineages in context. We focused on the nervous system, but the construct could be used in other tissues.

The current version of dBrainbow works well for labeling neurons from the same lineage in a common color because of the early expression of the Cre recombinase in the neuroblasts. Biological questions remain about how lineages develop in relation to one another. The lineages may act as functional units in neural circuits; understanding how they project and interact is key for testing this hypothesis. Some *GAL4* lines express in multiple lineages and dBrainbow is an efficient way to image individual lineages in them. For labeling individual neurons, a *GAL4* line that does not express throughout whole lineages can be chosen. Although the recombination to select a specific fluorescent protein occurs in the neuroblast, only the cells expressing *GAL4* produce this color. To subdivide the neurons in a lineage into different colors would require a truly inducible source of Cre recombinase. All of the existing *D. melanogaster* Cre recombinase reagents suffer from drawbacks including leaky expression, poor inducibility and/or toxicity. The development of better Cre recombinase reagents would be a great contribution to the field. We routinely compare the total expression pattern of *GAL4* labeled with *UAS-dBrainbow* to the expression pattern revealed by cytoplasmic *UAS-EGFP* (Bloomington 1521) or *UAS-mCD8-GFP* to determine what fraction of the neurons we are detecting and whether their projections appear normal. With appropriate controls, we obtained biologically interesting results with the existing *hs-Cre* lines.

One of the next major goals in *D. melanogaster* neuroanatomy is to map each individual neuron in the fly brain. Techniques such as dBrainbow facilitate this by speeding up imaging (multiple individual neurons can be seen in each brain) but also because labeling one neuron in the context of others makes assigning it to a class or type less ambiguous.

METHODS

Methods and any associated references are available in the online version of the paper at <http://www.nature.com/naturemethods/>.

Accession codes. GenBank: JF267350 (*dBrainbow*).

Note: Supplementary information is available on the Nature Methods website.

ACKNOWLEDGMENTS

We thank A. Arnold, E. Shumsky and A. Soell for help with imaging and spectral separation; B. Pfeiffer, A. Nern and G. Rubin (Janelia Farm Research Campus)

for sharing vectors and recombinase lines before publication and for the gift of *R12D05-GAL4*; V. Hartenstein, B. Gerber, T. Lee, B. Baker and P. Keller for helpful discussions about biological applications of dBrainbow; S. Albin, A. Seeds and E. Hooper for scientific discussion of the project; D. Grover for statistical advice; and K. Basler, R. Yagi and C. Lehner (University of Zurich) and M. Siegal (New York University) for additional Cre lines.

AUTHOR CONTRIBUTIONS

S.H. designed and performed cloning, tested constructs in S2 cells and made the figures. P.C. performed the fly genetics, immunohistochemistry and confocal imaging. C.E.M. generated and analyzed the subesophageal ganglion and proboscis data. D.H. generated the recombinant fly stocks. L.L.L. advised on selection of fluorescent proteins, construct design and the conversion from endogenous fluorescence to antibody. J.H.S. conceived the project, cloned initial test constructs and wrote the paper with help from S.H., P.C., C.E.M. and L.L.L.

COMPETING FINANCIAL INTERESTS

The authors declare no competing financial interests.

Published online at <http://www.nature.com/naturemethods/>.

Reprints and permissions information is available online at <http://npg.nature.com/reprintsandpermissions/>.

1. Lichtman, J.W., Livet, J. & Sanes, J.R. A technicolour approach to the connectome. *Nat. Rev. Neurosci.* **9**, 417–422 (2008).
2. Simpson, J.H. Mapping and manipulating neural circuits in the fly brain. *Adv. Genet.* **65**, 79–143 (2009).
3. Bellen, H.J., Tong, C. & Tsuda, H. 100 years of *Drosophila* research and its impact on vertebrate neuroscience: a history lesson for the future. *Nat. Rev. Neurosci.* **11**, 514–522 (2010).
4. Lai, S.L. & Lee, T. Genetic mosaic with dual binary transcriptional systems in *Drosophila*. *Nat. Neurosci.* **9**, 703–709 (2006).
5. Yu, H.H., Chen, C.H., Shi, L., Huang, Y. & Lee, T. Twin-spot MARCM to reveal the developmental origin and identity of neurons. *Nat. Neurosci.* **12**, 947–953 (2009).
6. Livet, J. *et al.* Transgenic strategies for combinatorial expression of fluorescent proteins in the nervous system. *Nature* **450**, 56–62 (2007).
7. Sakaue-Sawano, A. *et al.* Visualizing spatiotemporal dynamics of multicellular cell-cycle progression. *Cell* **132**, 487–498 (2008).
8. Ai, H.W., Shaner, N.C., Cheng, Z., Tsien, R.Y. & Campbell, R.E. Exploration of new chromophore structures leads to the identification of improved blue fluorescent proteins. *Biochemistry* **46**, 5904–5910 (2007).
9. Busch, S., Selcho, M., Ito, K. & Tanimoto, H. A map of octopaminergic neurons in the *Drosophila* brain. *J. Comp. Neurol.* **513**, 643–667 (2009).
10. Masse, N.Y., Turner, G.C. & Jefferis, G.S. Olfactory information processing in *Drosophila*. *Curr. Biol.* **19**, R700–R713 (2009).
11. Jefferis, G.S., Marin, E.C., Stocker, R.F. & Luo, L. Target neuron prespecification in the olfactory map of *Drosophila*. *Nature* **414**, 204–208 (2001).
12. Marin, E.C., Jefferis, G.S., Komiyama, T., Zhu, H. & Luo, L. Representation of the glomerular olfactory map in the *Drosophila* brain. *Cell* **109**, 243–255 (2002).
13. Wong, A.M., Wang, J.W. & Axel, R. Spatial representation of the glomerular map in the *Drosophila* protocerebrum. *Cell* **109**, 229–241 (2002).
14. Lai, S.L., Awasaki, T., Ito, K. & Lee, T. Clonal analysis of *Drosophila* antennal lobe neurons: diverse neuronal architectures in the lateral neuroblast lineage. *Development* **135**, 2883–2893 (2008).
15. Siegal, M.L. & Hartl, D.L. Transgene Coplacement and high efficiency site-specific recombination with the Cre/loxP system in *Drosophila*. *Genetics* **144**, 715–726 (1996).
16. Heidmann, D. & Lehner, C.F. Reduction of Cre recombinase toxicity in proliferating *Drosophila* cells by estrogen-dependent activity regulation. *Dev. Genes Evol.* **211**, 458–465 (2001).
17. Jefferis, G.S. *et al.* Comprehensive maps of *Drosophila* higher olfactory centers: spatially segregated fruit and pheromone representation. *Cell* **128**, 1187–1203 (2007).
18. Ito, K. & Awasaki, T. Clonal unit architecture of the adult fly brain. in *Brain Development in Drosophila melanogaster* Vol. 628. (ed., G.M. Technau) 137–159 (Landes Bioscience and Springer Science and Business Media, 2008).
19. Lee, T., Lee, A. & Luo, L. Development of the *Drosophila* mushroom bodies: sequential generation of three distinct types of neurons from a neuroblast. *Development* **126**, 4065–4076 (1999).
20. Siegal, M.L. & Hartl, D.L. Application of Cre/loxP in *Drosophila*. Site-specific recombination and transgene coplacement. *Methods Mol. Biol.* **136**, 487–495 (2000).

21. Yagi, R., Mayer, F. & Basler, K. Refined LexA transactivators and their use in combination with the *Drosophila* Gal4 system. *Proc. Natl. Acad. Sci. USA* **107**, 16166–16171 (2010).
22. de Velasco, B. *et al.* Specification and development of the pars intercerebralis and pars lateralis, neuroendocrine command centers in the *Drosophila* brain. *Dev. Biol.* **302**, 309–323 (2007).
23. Potter, C.J. & Luo, L. Octopamine fuels fighting flies. *Nat. Neurosci.* **11**, 989–990 (2008).
24. Busch, S. & Tanimoto, H. Cellular configuration of single octopamine neurons in *Drosophila*. *J. Comp. Neurol.* **518**, 2355–2364 (2010).
25. Manoli, D.S. *et al.* Male-specific fruitless specifies the neural substrates of *Drosophila* courtship behaviour. *Nature* **436**, 395–400 (2005).
26. Demir, E. & Dickson, B.J. Fruitless splicing specifies male courtship behavior in *Drosophila*. *Cell* **121**, 785–794 (2005).
27. Kimura, K., Hachiya, T., Koganezawa, M., Tazawa, T. & Yamamoto, D. Fruitless and doublesex coordinate to generate male-specific neurons that can initiate courtship. *Neuron* **59**, 759–769 (2008).
28. Cachero, S., Ostrovsky, A.D., Yu, J.Y., Dickson, B.J. & Jefferis, G.S. Sexual dimorphism in the fly brain. *Curr. Biol.* **20**, 1589–1601 (2010).
29. Yu, J.Y., Kanai, M.I., Demir, E., Jefferis, G.S. & Dickson, B.J. Cellular organization of the neural circuit that drives *Drosophila* courtship behavior. *Curr. Biol.* **20**, 1602–1614 (2010).
30. Isono, K. & Morita, H. Molecular and cellular designs of insect taste receptor system. *Front. Cell Neurosci.* **4**, 20 (2010).
31. Vosshall, L.B. & Stocker, R.F. Molecular architecture of smell and taste in *Drosophila*. *Annu. Rev. Neurosci.* **30**, 505–533 (2007).
32. Rajashekhar, K.P. & Singh, R.N. Neuroarchitecture of the tritocerebrum of *Drosophila melanogaster*. *J. Comp. Neurol.* **349**, 633–645 (1994).
33. Tissot, M., Gendre, N. & Stocker, R.F. *Drosophila* P[Gal4] lines reveal that motor neurons involved in feeding persist through metamorphosis. *J. Neurobiol.* **37**, 237–250 (1998).
34. Gordon, M.D. & Scott, K. Motor Control in a *Drosophila* Taste Circuit. *Neuron* **61**, 373–384 (2009).
35. Miller, A. The internal anatomy and histology of the imago of *Drosophila melanogaster*. in *Biology of Drosophila*. (ed., Demerec, M.) 420–534 (Cold Spring Harbor Laboratory Press, Cold Spring Harbor, New York, USA, 1950).

ONLINE METHODS

Molecular biology and *D. melanogaster* genetics. DNA encoding the *D. melanogaster* codon-optimized fluorescent proteins was ordered from DNA2.0. The fluorescent proteins were then cloned into shuttle vectors carrying cellular localization signals. Epitope tags³⁶ were added on PCR primers synthesized by IDT. The vectors were modular so individual components can be exchanged by restriction digests. The final constructs were cloned into the PhiC31 integration vector JFRC-MUH³⁷ for generating *D. melanogaster* transformants at *atp2* and *atp40* sites³⁸ (Genetic Services, Inc.). The *lox* sites used were *loxP*, *lox2272* and *lox5171* (refs. 15,39). We built *hs-Cre*; *enhancer-GAL4* stocks and crossed virgin females to *UAS-dBrainbow* males. The *hs-Cre* lines were from the Bloomington Stock Center (766 and 851). The *hs-Cre* construct contains a *mos1* enhancer element thought to drive ubiquitous early expression^{15,16}. Unless noted, we reared fly crosses at 18 °C and did not heat-shock them. We saw no increase in sparseness of the color distribution with heat-shock of adult flies. Heat shocks early in development caused toxicity rather than an increase in neuronal labeling. Additional fly stocks used were *Fruitless GAL4* (ref. 25), *GH146-GAL4* (ref. 40) (Bloomington 30026), *TDC2-GAL4* (ref. 41), *OK107-GAL4* (ref. 42) and *R12D05-GAL4* (gift of G. Rubin, Janelia Farm Research Campus).

Immunohistochemistry. Adult brain and ventral nerve cords were dissected with Inox 5 forceps on Sylgard dishes loosely following established protocols⁴³. For endogenous fluorescence analysis, 3–7-day-old adult females were dissected in 1× PBS (pH 7) and fixed rotating at room temperature (~21 °C) with 2% paraformaldehyde (Sigma) for 1 h. Samples were then washed 3× for 20 min each with PAT (1× PBS, 1% BSA (Sigma) and 0.5% Triton X-100 (Sigma)). Tissue was rinsed in 1× PBS and then mounted in VectaShield (Vector Laboratories) on glass slides with two transparent reinforcement rings as spacers. Before imaging, mounted samples were kept at room temperature for 1 h or stored at –20 °C. For antibody staining, 3–7-day-old female flies were dissected in 1× PBS. (For proboscis staining, the proboscis segments were cut into separate pieces to allow antibody penetration.) Tissue was fixed with 2% paraformaldehyde (Sigma) overnight (~16 h) at 4 °C with gentle rocking. Samples were washed 3× for 20 min each with PAT and then blocked with 3% normal goat serum (NGS; BioSource) in PAT for 1 h at room temperature. Primary antibody incubations were performed overnight at 4 °C, nutating in 500 µl PAT plus NGS with the following dilutions: rabbit anti-GFP (1:500; Invitrogen, A11122), mouse anti-Myc (1:50; Developmental Studies Hybridoma Bank, 9E10) and rat anti-HA (1:100; Roche, 11867423001). Samples were washed 3× for 20 min each with PAT and then incubated overnight with goat secondary antibodies from Molecular Probes/Invitrogen⁴⁴: Alexa Fluor 488 anti-rabbit (1:500; A11034), Alexa Fluor 568 anti-mouse (1:500; A11031) and Alexa Fluor 633 anti-rat (1:500; A21094). Samples were washed again 3× for 20 min each with PAT, rinsed with 1× PBS and mounted in VectaShield. Before imaging, mounted samples were kept at room temperature for 1 h or stored –20 °C. The majority of the crosses were not heat-shocked as *hs-Cre* provides enough baseline expression to generate recombination events, but the *R12D05-GAL4* crosses were heat-shocked for 1 h at 37 °C at 24 h after egg laying. We find that the cross-absorbed secondary

antibodies and the Triton concentrations are critical for obtaining clean fluorescent signals with dBrainbow.

S2 cell culture. S2 cells were grown in Schneider's *D. melanogaster* medium containing heat-inactivated FBS (Invitrogen) and 10 µg ml^{–1} penicillin and streptomycin, pelleted and resuspended to a density of 10⁶ cells ml^{–1} in 6-well plates (10⁶ cells per well). Cells in each well were transfected with 1.25 µg of DNA purified with a QIAprepSpin Maxi kit using the Qiagen Effectene Transfection kit. *Ubiquitin-GAL4* was used to drive *UAS-dBrainbow* and different fluorescent protein constructs. For transfections of *UAS-dBrainbow* constructs 150 ng *hs-Cre* DNA was transfected with 1 µg *UAS-dBrainbow* DNA and 100 ng *Ubiquitin-GAL4* DNA. For each transfection we used 1 µg of fluorescent protein-encoding DNA, 100 ng *Ubiquitin-GAL4* DNA and 150 ng of *pcDNA3* to reach a total DNA concentration of 1.25 µg well^{–1}. The cells were then incubated for 2 d at 25 °C and analyzed under a confocal microscope.

Confocal imaging. Confocal images were taken on a Zeiss 510 confocal microscope (Zen 2009 software) using a 20× Plan-Apochromat 0.8 numerical aperture (NA) lens with the following settings: 1 µm *z*-dimension steps, sequential scanning, 1,024 × 1,024 pixels, 12-bit data, scan speed 7 and bidirectional scanning with auto-*z*-dimension correction. We also imaged endogenous fluorescence and antibody-stained samples with a 40× Plan-Apochromat 1.3 NA oil-immersion lens on a Zeiss 710 confocal microscope (Zen 2008 software) to improve the spectral separation using wavelength-specific metadetectors. The critical step to achieve completely separate detection of each fluorescent protein or Alexa Fluor dye was to scan sequentially: EBFP or Cerulean for the endogenous version was imaged first with the 458 nm argon laser line and 470–500 nm band-pass filters, then mKO2 or Alexa Fluor 568 with DPSS 561 nm line and 575–615 nm band-pass filter. Lastly, GFP or Alexa Fluor 488 was imaged with a 488-nm argon laser and 505–550 nm band-pass filter. For the antibody version, Alexa Fluor 633 was visualized with the HeNe 633 nm laser line and 650 nm long-pass filter. We carefully checked that there was no bleedthrough with these settings when we imaged the constructs expressing each fluorescent protein individually. Original confocal image stacks are available upon request.

36. Brizzard, B. Epitope tagging. *Biotechniques* **44**, 693–695 (2008).
37. Pfeiffer, B.D. *et al.* Tools for neuroanatomy and neurogenetics in *Drosophila*. *Proc. Natl. Acad. Sci. USA* **105**, 9715–9720 (2008).
38. Groth, A.C., Fish, M., Nusse, R. & Calos, M.P. Construction of transgenic *Drosophila* by using the site-specific integrase from phage phiC31. *Genetics* **166**, 1775–1782 (2004).
39. Rodin, S. & Georgiev, P. Handling three regulatory elements in one transgene: combined use of cre-lox, FLP-FRT, and I-SceI recombination systems. *Biotechniques* **39**, 871–876 (2005).
40. Stocker, R.F., Heimbeck, G., Gendre, N. & de Belle, J.S. Neuroblast ablation in *Drosophila* P[GAL4] lines reveals origins of olfactory interneurons. *J. Neurobiol.* **32**, 443–456 (1997).
41. Cole, S.H. *et al.* Two functional but noncomplementing *Drosophila* tyrosine decarboxylase genes: distinct roles for neural tyramine and octopamine in female fertility. *J. Biol. Chem.* **280**, 14948–14955 (2005).
42. Connolly, J.B. *et al.* Associative learning disrupted by impaired Gs signaling in *Drosophila* mushroom bodies. *Science* **274**, 2104–2107 (1996).
43. Wu, J.S. & Luo, L. A protocol for dissecting *Drosophila melanogaster* brains for live imaging or immunostaining. *Nat. Protoc.* **1**, 2110–2115 (2006).
44. Panchuk-Voloshina, N. *et al.* Alexa dyes, a series of new fluorescent dyes that yield exceptionally bright, photostable conjugates. *J. Histochem. Cytochem.* **47**, 1179–1188 (1999).